Biogeosciences Discuss., 11, 12799–12831, 2014
www.biogeosciences-discuss.net/11/12799/2014/
doi:10.5194/bgd-11-12799-2014

Biogeosciences Discussions
Open Access

Secondary calcification and dissolution respond differently to future ocean conditions

N. J. Silbiger and M. J. Donahue

University of Hawai'i at Mānoa, Hawai'i Institute of Marine Biology, P.O. Box 1346, Kāne'ohe, Hawai'i, 96744, USA

Received: 8 August 2014 – Accepted: 13 August 2014 – Published: 2 September 2014

Correspondence to: N. J. Silbiger (silbiger@hawaii.edu)

Published by Copernicus Publications on behalf of the European Geosciences Union.

Abstract

Climate change threatens both the accretion and erosion processes that sustain coral reefs. Secondary calcification, bioerosion, and reef dissolution are integral to the structural complexity and long-term persistence of coral reefs, yet these processes have received less research attention than reef accretion by corals. In this study, we use climate scenarios from RCP8.5 to examine the combined effects of rising ocean acidity and SST on both secondary calcification and dissolution rates of a natural coral rubble community using a flow-through aquarium system. We found that secondary reef calcification and dissolution responded differently to the combined effect of pCO_2 and temperature. Calcification had a non-linear response to the combined effect of pCO_2-temperature: the highest calcification rate occurred slightly above ambient conditions and the lowest calcification rate was in the highest pCO_2-temperature condition. In contrast, dissolution increased linearly with pCO_2-temperature. The rubble community switched from net calcification to net dissolution at +272 µatm pCO_2 and 0.84 °C above ambient conditions, suggesting that rubble reefs may shift from net calcification to net dissolution before the end of the century. Our results indicate that dissolution may be more sensitive to climate change than calcification, and that calcification and dissolution have different functional responses to climate stressors, highlighting the need to study the effects of climate stressors on both calcification and dissolution to predict future changes in coral reefs.

1 Introduction

In 2013, atmospheric carbon dioxide (CO_2(atm)) reached an unprecedented milestone of 400 ppm (Tans and Keeling, 2013), and this rising $CO_{2(atm)}$ is increasing sea-surface temperature (SST) and ocean acidity (Caldeira and Wickett, 2003; Cubasch et al., 2013; Feely et al., 2004). Global SST has increased by 0.78 °C since pre-industrial times (Cubasch et al., 2013), and it is predicted to increase by another 0.8–5.7 °C by

BGD
11, 12799–12831, 2014

the end of this century (Meinshausen et al., 2011; Van Vuuren et al., 2008; Rogelj et al., 2012). The Hawai'i Ocean Time-series detected a 0.075 decrease in mean annual pH at Station ALOHA over the past 20 yr (Doney et al., 2009) and there have been similar trends at stations around the world including the Bermuda Atlantic Time-series and the European Station for Time-series Observations in the ocean (Drupp et al., 2013). pH is expected to drop by an additional 0.14–0.35 pH units by the end of the 21st century (Bopp et al., 2013). All marine ecosystems are at risk from rising SST and decreasing pH (Doney et al., 2009; Hoegh-Guldberg et al., 2007; Hoegh-Guldberg and Bruno, 2010), but coral reefs are particularly vulnerable to these stressors (reviewed in Hoegh-Guldberg et al., 2007).

Corals create the structurally complex calcium carbonate ($CaCO_3$) foundation of coral reef ecosystems. This structural complexity is at risk from climate-driven shifts from high-complexity, branched coral species to mounding and encrusting growth forms (Fabricius et al., 2011) and from increases in the natural processes of reef destruction, including bioerosion and dissolution (Wisshak et al., 2012, 2013; Tribollet et al., 2006). While substantial research attention has focused on the response of reef-building corals to climate change (reviewed in Hoegh-Guldberg et al., 2007; Fabricius, 2005; Pandolfi et al., 2011), secondary calcification (calcification by non-coral invertebrates and calcareous algae), bioerosion, and reef dissolution that are integral to maintaining the structural complexity and net growth of coral reefs has received less attention (Andersson and Gledhill, 2013; Andersson et al., 2011; Andersson and Mackenzie, 2012). Coral reefs will only persist if constructive reef processes (growth by corals and secondary calcifiers) exceed destructive reef processes (bioerosion and dissolution). In this study, we examine the combined effects of rising ocean acidity and SST on both calcification and dissolution rates of a natural community of secondary calcifiers and bioeroders.

Recent laboratory experiments have focused on the response of individual taxa of bioeroders or secondary calcifiers to climate stressors. For example, studies have specifically addressed the effects of rising ocean acidity and/or temperature on bioero-

BGD
11, 12799–12831, 2014

sion by a *Clionid* sponge (Wisshak et al., 2012, 2013; Fang et al., 2013) and a community of photosynthesizing microborers (Tribollet et al., 2009; Reyes-Nivia et al., 2013). These studies found that bioerosion increased under future climate change scenarios. Several studies have focused on tropical calcifying algae and have found decreased calcification (Semesi et al., 2009; Johnson et al., 2014; Comeau et al., 2013; Jokiel et al., 2008; Kleypas and Langdon, 2006) and increased dissolution (Diaz-Pulido et al., 2012) with increasing ocean acidity and/or SST. However, the bioeroding community is extremely diverse and can interact with the surrounding community of secondary calcifiers: for example, crustose coralline algae (CCA) can inhibit internal bioerosion (White, 1980; Tribollet and Payri, 2001). To understand the combined response of bioeroders and secondary calcifiers, we take a community perspective. We examine the synergistic effects of rising SST and ocean acidity, modeled after the Representative Concentration Pathway (RCP) 8.5 climate scenario (Van Vuuren et al., 2011; Meinshausen et al., 2011), on a natural community of secondary calcifiers and bioeroders. Using the total alkalinity anomaly technique, we test for net changes in calcification during the day and dissolution (most of which is caused by bioeroders; Andersson and Gledhill, 2013), at night. RCP scenarios are the emissions scenarios that were used in the most recent Intergovernmental Panel on Climate Change (IPCC) report (Cubasch et al., 2013). The RCP8.5 scenario predicts that temperature will likely increase by 3.8–5.7 °C (Rogelj et al., 2012) and atmospheric CO_2 will increase by 557 ppm the year 2100 (Meinshausen et al., 2011). We chose to use the RCP8.5 scenario because the current CO_2 concentrations are tracking just above what this scenario predicts (Sanford et al., 2014). While prior studies have focused on the contributions of individual community members, here, we test the community response to the predicted RCP8.5 climate scenario and measure both calcification and dissolution rates.

BGD
11, 12799–12831, 2014

2 Materials and methods

2.1 Collection site

All collections were made on the windward side of Moku o Lo'e (Coconut Island) in Kāne'ohe Bay, Hawai'i adjacent to the Hawai'i Institute of Marine Biology. This fringing reef is dominated by *Porites compressa* and *Montipora capitata*, with occasional colonies of *Pocillopora damicornis*, *Fungia scutaria*, and *Porites lobata*. Kāne'ohe Bay is a protected, semi-enclosed embayment; the residence time can be > 1 month long in the protected southern portion of the Bay (Lowe et al., 2009a,b) that is coupled with a high daily variance in pH (Guadayol et al., 2014). The wave action is minimal (Smith et al., 1981; Lowe et al., 2009a,b) and currents are relatively slow (5 cm s^{-1} maximum) and wind-driven (Lowe et al., 2009a,b).

2.2 Sample collection

We collected pieces of dead *Porites compressa* coral skeleton (hereafter, referred to as rubble) as representative communities of bioeroders and secondary calcifiers. Rubble was collected with a hammer and chisel from a shallow reef flat (~ 1 m depth) in November 2012. Only pieces of rubble without any live coral were collected. The average (±SE) skeletal density of the rubble was 1.53 ± 0.012 g cm^{-3} (n = 85). The rubble community in Kāne'ohe Bay is comprised of secondary calcifiers, including CCA from the genera *Hydrolithon*, *Sporolithon*, and *Peyssonnelia* and non-coral calcifying invertebrates (e.g. boring bivalves (*Lithophaga fasciola* and *Barbatia divaricate*), oysters (*Crassostrea gigas*), and small crustaceans); filamentous and turf algae; and internal bioeroders, including boring bivalves (*L. fasciola* and *B.divaricate*), sipunculids (*Aspidosiphon elegans*, *Lithacrosiphon cristatus*, *Phascolosoma perlucens*, and *Phascolosoma stephensoni*), phoronids (*Phoronis ovalis*), sponges (*Cliona* spp.) and a diverse assemblage of polychaetes (White, 1980). All rubble was combined after collection and

BGD
11, 12799–12831, 2014

maintained in a 100 L flow-through tank with ambient seawater from Kāne'ohe Bay until random assignment to treatments.

2.3 Experimental design

The Hawai'i Institute of Marine Biology (HIMB) hosts a mesocosm facility with flow-through seawater from Kāne'ohe Bay and controls for light, temperature, pCO_2, and flow rate. The facility is comprised of 24 experimental aquaria split between four racks; each rack has a 150 L header tank which feeds 6 experimental aquaria, each 50 L in volume (Fig. 1).

Before adding rubble to the experimental aquaria, we collected pH, total alkalinity (TA), temperature, and salinity from each aquarium during light and dark conditions to demonstrate the stability of the system without any rubble present (Table 1). We then conducted "control" and "treatment" experiments to determine how RCP8.5 predictions affect daytime calcification and nighttime dissolution rates in a natural rubble community. The first "control experiment" characterized baseline calcification and dissolution in each aquarium caused by differences in rubble communities. In the second "treatment experiment", we manipulated pCO_2 and temperature to simulate four climate scenarios (pre-industrial, present day, 2050, and 2100) and tested the response of calcification and dissolution.

Approximately 1.2 L of rubble (4–5 pieces of approximately equal size) were placed in each of the 24 experimental aquaria and acclimated to tank conditions in ambient seawater for three days. On the fourth day, we performed the control experiment, calculating daytime calcification and nighttime dissolution for rubble in the ambient seawater using the TA anomaly technique (Smith and Key, 1975). The next day we manipulated seawater pCO_2 and temperature to replicate four climate scenarios for the treatment experiment (Table 1): pre-industrial (-1 ± 0.057 °C and -205 ± 11.9 µatm), present day (natural Kāne'ohe Bay seawater 24.8 ± 0.09 °C, 614 ± 15.6 µatm), 2050 ($+1.4 \pm 0.09$ °C and $+255 \pm 31$ µatm), and 2100 ($+2.4 \pm 0.08$ and $+433 \pm 40$ µatm). Note that all changes in temperature and pCO_2 were made relative to present day Kāne'ohe Bay seawa-

BGD
11, 12799–12831, 2014

ter conditions: pCO_2 in Kāne'ohe Bay is consistently high relative to the open ocean and can range from 196–976 µatm in southern Kāne'ohe bay depending on conditions (Drupp et al., 2013). The yearly average pCO_2 at our collection site ranged from 565–675 µatm (Silbiger et al., 2014). After an acclimation time of seven days, we sampled the treatment experiment, calculating daytime calcification and nighttime dissolution over a 24 h period.

During both experiments, TA, pH, salinity, temperature, and dissolved inorganic nutrient (DIN) samples were collected every 12 h over a 24 h period (total of three times): just before lights-on in the morning (time 1) and just before lights-off at night (time 2) to capture light conditions, and then again before lights-on the next morning (time 3) to capture dark conditions. Flow into each aquarium was monitored and adjusted every three hours to ensure a consistent flow rate over the 24 h experiment. We calculated net ecosystem calcification and dissolution using a simple box model (Andersson et al., 2009) and normalized all our calculations to the surface area of the rubble in each tank. Surface area of the rubble was calculated using the wax dipping technique (Stimson and Kinzie III, 1991) at the end of the experiment.

2.4 Laboratory Set-up

The mesocosm facility (Fig. 1) is supplied with ambient seawater from Kāne'ohe Bay, which is filtered through a sand filter, passed through a water chiller (Aqualogic Multi Temp MT-1 Model # 2TTB3024A1000AA), and then fed into one of the four header tanks. pCO_2 was manipulated using a CO_2 gas blending system (see Fangue et al., 2010; Johnson and Carpenter, 2012). Each target pCO_2 concentration was created by mixing CO_2-free atmospheric air with pure CO_2 using mass flow controllers (C100L Sierra Instruments). Output pCO_2 was analyzed using a calibrated infrared CO_2 analyzer (A151, Qubit Systems). CO_2 mixtures were then bubbled into one of the four header tanks and water from each individual header tank fed into the six individual treatment aquaria (Fig. 1). The pCO_2 in each treatment aquarium was estimated with CO2SYS (Van Heuven et al., 2009) using pH and TA as the parameters.

BGD
11, 12799–12831, 2014

Temperature was manipulated in each treatment aquarium using dual-stage temperature controllers (Aqualogic TR115DN). The temperature was continuously monitored with temperature loggers (TidbiT v2 Water Temperature Data Logger, sampling every 20 min) and point measurements were taken during every sampling period with a handheld digital thermometer (Traceable Digital Thermometer, Thermo Fisher Scientific; precision = 0.001 °C). Light was controlled by positioning an oscillating pendant metal-halide light (250 W) over a set of three aquaria and was programmed to emit an equal amount of light to each tank (~500 µE of light). Lights were set to a 12 : 12 h photoperiod and were monitored using a LI-COR spherical quantum PAR sensor. Flow rate was maintained at 115±1 mL min^{-1}, resulting in a residence time of 7.3 ± 0.07 h per tank. Each aquarium was equipped with a submersible powerhead pump (Sedra KSP-7000 powerhead) to ensure that the tank was well-mixed.

2.5 Seawater chemistry

All sample collection and storage vials were cleaned in a 10 % HCl bath for 24 h and rinsed three times with MilliQ water before use and rinsed three times with sample water during sample collection and processing.

2.5.1 Total alkalinity

Duplicate TA samples were collected in 300 mL borosilicate sample containers with glass stoppers. Each sample was preserved with 100 µL of 50 % saturated $HgCl_2$ and analyzed within 3 days using open cell potentiometric titrations on a Mettler T50 autotitrator (Dickson et al., 2007). A Certified Reference Material (CRM – Reference Material for Oceanic CO_2 Measurements, A. Dickson, Scripps Institution of Oceanography) was run at the beginning of each sample set to ensure the accuracy of the titrator. Our accuracy was better than ±0.8 %, and our precision was 3.55 µ Eq (measured as standard deviation of the duplicate water samples).

BGD
11, 12799–12831, 2014

2.5.2 pH_t (total scale)

Duplicate pH_t samples were collected in 20 mL borosilicate glass vials, brought to a constant temperature of 25 °C in a water bath, and immediately analyzed using an m-cresol dye addition spectrophotometric technique. Accuracy of the pH was tested against a Tris buffer of known pH_t from the Dickson Lab at Scripps Institution of Oceanography (Dickson et al., 2007). Our accuracy was better than ±0.04 % and the precision was 0.004 pH units (measured as standard deviation of the duplicate water samples). In situ pH and the remaining carbonate parameters were calculated using CO2SYS (Van Heuven et al., 2009) with the following measured parameters: pH_t, TA, temperature, and salinity. The K1K2 apparent equilibrium constants were from Mehrbach (1973) and refit by Dickson and Millero (1987) and HSO_4 dissociation constants were taken from Uppström (1974) and Dickson (1990).

2.5.3 Salinity

Duplicate salinity samples were analyzed on a Portasal 8410 portable salinometer which was calibrated with an OSIL IAPSO standard (accuracy = ±0.003 psu, precision = ±0.0003 psu).

2.5.4 Nutrients

Nutrient samples were collected with 60 mL plastic syringes and immediately filtered through combusted 25 mm glass fiber filters (GF/F 0.7 µm) and transferred into 50 mL plastic centrifuge tubes. Nutrient samples were frozen and later analyzed for $Si(OH)_4$, NO_3^-, NO_2^-, NH_4^+, and PO_4^{3-} on a Seal Analytical AA3 HR Nutrient Analyzer at the UH SOEST Lab for Analytical Chemistry.

BGD
11, 12799–12831, 2014

2.6 Measuring net ecosystem calcification

We assumed that the mesocosms were well mixed systems; thus, we calculated net ecosystem calcification and net communtity photosynthesis following the simple box model presented in Andersson et al. (2009). TA was first normalized to a constant salinity (35 psu) and to (DIN) to account for changes in TA due to evaporation and photosynthesis/respiration, respectively. Net ecosystem calcification, or G, was calculated using the following equation:

$$G = \left[F_{\mathrm{TAin}} - F_{\mathrm{TAout}} - \frac{\mathrm{dTA}}{\mathrm{d}t}\right]/2 \quad (1)$$

F_{TAin} is the rate of TA flowing into the aquaria, F_{TAout} is the rate of TA flowing out of the aquaria, and, $\frac{\mathrm{dTA}}{dt}$ is the change in TA in the aquaria per unit time in mmol $CaCO_3$ m^{-2} h^{-1}. The equation is divided by two because one mole of $CaCO_3$ is precipitated or dissolved for every two moles of TA removed or added to the water column. Here, G represents the sum of all the calcification processes minus the sum of all the dissolution processes in mmol $CaCO_3$ m^{-2} h^{-1}; thus, all positive numbers are net calcification and all negative numbers are negative net calcification (i.e., net dissolution). Net daytime calcification (G_{day}) is calculated from the first 12 h sampling period in the light, net nightime dissolution (G_{night}) is calculated from the second 12 h sampling period in the dark, and total net calcification (G_{net}) is calculated from the full 24 h cycle (G_{day} + G_{night}). All rates are presented as mmol $CaCO_3$ m^{-2} d^{-1}.

2.7 Measuring net community production and respiration

Net community production (NCP) was calculated by measuring changes in DIC (Gattuso et al., 1999). DIC was normalized to a constant salinity (35 psu) to account for any

BGD
11, 12799–12831, 2014

evaporation over the 24 h period. We used a simple box model to calculate NCP:

$$\mathrm{NCP} = \left[F_{\mathrm{DICin}} - F_{\mathrm{DICout}} - \frac{\mathrm{dDIC}}{\mathrm{d}t}\right] - G \quad (2)$$

F_{DICin}, F_{DICout}, and $\frac{\mathrm{dDIC}}{\mathrm{d}t}$ are the rates of DIC flowing into the aquaria, flowing out of the aquaria, and the change in DIC in the aquaria per unit time in mmol C m^{-2} h^{-1}, respectively. To measure NCP, we subtract G to remove any change in carbon due to inorganic processes. NCP represents the sum of all the photynthetic processes minus the sum of all the respiration processes, thus all positive numbers are net photosynthesis and all negative numbers are negative net photosynthesis (i.e., net respiration). All rates are presented as mmol C m^{-2} d^{-1}.

2.8 Statistical analysis

Each aquarium contained a slightly different rubble community because of the randomization of rubble pieces to each treatment. To ensure there were no systematic differences in rubble communities between racks (rack effects) before the experimental treatments were applied, we tested for differences in G_{day}, G_{night}, and G_{net} between racks in the control experiment using an ANOVA.

In the treatment experiment, we first tested for feedbacks in carbonate chemistry due to the presence of rubble: using a paired t test, we compared the day–night difference in measured $p\mathrm{CO}_2$ in each aquarium with rubble, ($p\mathrm{CO}_2$, day – $p\mathrm{CO}_2$, night)$_{\mathrm{rubble}}$, and without rubble, ($p\mathrm{CO}_2$, day – $p\mathrm{CO}_2$, night)$_{\mathrm{no\ rubble}}$. Because of the near-continuous variation in $p\mathrm{CO}_2$ and temperature across treatments and the significant feedbacks in the water chemistry due to the presence of rubble (Figs. 2 and A1), a regression using the actual seawater condition was more informative than an ANOVA using the imposed seawater condition in testing relationships between net calcification (G) and treatment. Therefore, we used a regression to test for linear and non-linear relationships between day, night, and net calcification (G_{day}, G_{night}, and G_{net}) and our independent variable: change in $p\mathrm{CO}_2$ × temperature from background seawater conditions

BGD
11, 12799–12831, 2014

(hereafter, referred to as Standardized Climate Change). (Results using an ANOVA design are included as Supplement Fig. A2, Table A1). Standardized Climate Change was calculated as (Treatment Experiment $pCO_{2,i}$ × Temperature$_i$) – (Control Experiment $pCO_{2,i}$ × Temperature$_i$), where i represents an individual aquarium. A simple product was used because pCO_2 increased linearly with temperature (Fig. 2). We centered the data around the ambient conditions such that a value of 0 in the independent variable (Standardized Climate Change) corresponds to present day Kāne'ohe Bay conditions, a negative value corresponds to water that is colder and less acidic (pre-industrial) and a positive value corresponds to water that is warmer and more acidic (future conditions) compared to background seawater. For a simple test of nonlinearity response of calcification to standardized climate change, we included a quadratic term ((Standardized Climate Change)^2) in the model. For G_{day}, we used weighted regression (Fair, 1974) weight function: $w_i = 1/(1+|r_i|)$, where w_i = weight and r_i = residual to account for heteroscedasticity. All other data met assumptions for a linear regression. Lastly, we used a linear regression to test the relationship between G and NCP.

3 Results

3.1 Control experiment

For rubble in ambient seawater conditions, the average G_{day}, G_{night}, and G_{net} in the control experiment were 3.4±0.16 mmol m^{-2} d^{-1}, −2.4±0.15 mmol m^{-2} d^{-1}, and 0.96±0.20 mmol m^{-2} d^{-1}, respectively. There was no significant difference in G_{day} ($F_{3,23}$ = 0.68, p = 0.58), G_{night} ($F_{3,23}$ = 1.52, p = 0.24), or G_{net} ($F_{3,23}$ = 1.38, p = 0.28) between racks in the control experiment (Fig. A2).

BGD
11, 12799–12831, 2014

3.2 Treatment experiment

The rubble communities significantly altered the seawater chemistry, with higher pCO_2 than the applied pCO_2 manipulation, particularly at night (Fig. A1). The mean difference between day and night pCO_2 for all treatments was 134.4 ± 39 µatm without rubble and was 438.5 ± 163.9 µatm when rubble was present ($t_{23} = -7.23$, $p < 0.0001$; Fig. 2).

Standardized Climate Change was a significant predictor for G_{day}, G_{night}, and G_{net} (Table 2; Fig. 3). G_{day} had a non-linear relationship with Standardized Climate Change (Table 2, Fig. 3a), increasing to a threshold and then rapidly declining. G_{night}, however, had a strong linear relationship with Standardized Climate Change (Table 2; Fig. 3b), suggesting that joint increases in ocean pCO_2 and temperature will increase night time dissolution of coral rubble. Lastly, G_{net} had a strong negative relationship with Standardized Climate Change (Table 2; Fig. 3c) and the rubble community switched from net calcification to net dissolution at an increase in pCO_2 and temperature of 271.6 µatm and 0.84 °C, respectively.

G and NCP were significantly correlated ($p < 0.0001$, $R^2 = 0.85$; Figs. 4 and A3). In general, rubble that was net photosynthesizing was also net calcifying and rubble that was net respiring was also net dissolving. The exception was rubble experiencing the most extreme temperature-pCO_2 treatment, which was net respiring during the day while still holding a positive, yet very low, calcification rate.

4 Discussion

4.1 Carbonate chemistry feedbacks

The rubble communities in the aquaria significantly altered the seawater chemistry, particularly at night ($t_{23} = -7.23$, $p < 0.0001$; Fig. 2, Fig. A1). This day-night difference in seawater chemistry increased under more extreme climate scenarios, as predicted by Jury et al. (2013). This large diel swing in pCO_2 is not uncommon on shallow coral

BGD
11, 12799–12831, 2014

reef environments. pCO_2 ranged from 480 to 975 µatm over 24 h on a shallow reef flat adjacent to our collection site (Silbiger et al., 2014), and pCO_2 ranged from 450 to 742 µatm on a Moloka'i reef flat dominated by coral rubble (Yates and Halley, 2006). Here, pCO_2 had an average difference of 438 µatm between day and night with a range of 412 µatm in the pre-industrial treatment to 854 µatm in the most extreme pCO_2 × temperature treatments (Fig. 2). In our study, we incorporated these feedbacks into the statistical analysis by using the actual, sampled pCO_2 (and temperature) in each aquaria (Fig. 3) rather than using the intended pCO_2 (and temperature) treatments in an ANOVA (Table A1, Fig. A4), better reflecting the pCO_2 experienced by organisms in each aquarium.

4.2 Calcification and dissolution in a high CO_2 and temperature environment

Our results suggest that as pCO_2 and temperature increase over time, rubble reefs may shift from net calcification to net dissolution. In our study, this tipping point occurred at a pCO_2 and temperature increase of 271.6 µatm and 0.84 °C. Further, our results showed that G_{day} and G_{night} in a natural coral rubble community have different functional responses to changing pCO_2 and temperature (Fig. 3). The ranges in G_{day} and G_{night} in our aquaria were similar to in situ rates on Hawaiian rubble reefs. Yates and Halley (2006) saw G_{day} values between 0.26 to 0.98 mmol $CaCO_3$ m^{-2} h^{-1} and G_{night} values between −0.2 to −3.0 mmol $CaCO_3$ m^{-2} h^{-1} on a Moloka'i reef flat with only coral rubble. G_{day} and G_{night} in our experiment ranged from 0.16 to 0.78 and −0.10 to −0.87 mmol $CaCO_3$ m^{-2} h^{-1}, respectively, across all treatment conditions. The higher dissolution rates in the in situ study by Yates and Halley (2006) are likely due to dissolution in the sediment, which was not present in our study.

G_{day} had a non-linear response to Standardized Climate Change. G_{day} increased with pCO_2 × temperature until slightly above ambient conditions, and then decreased under more extreme climate conditions (Fig. 3a). This mixed response, increasing and then decreasing with Standardized Climate Change, is reflected in prior experiments.

BGD
11, 12799–12831, 2014

We suggest two possible mechanisms to explain why calcification increases in slightly higher pCO_2 × temperature than ambient conditions. (1) Some calcifiers can maintain and even increase their calcification rates in acidic conditions (Kamenos et al., 2013; Findlay et al., 2011; Rodolfo-Metalpa et al., 2011; Martin et al., 2013) by either modifying their local pH environment (Hurd et al., 2011) or partitioning their energetic resources towards calcification (Kamenos et al., 2013). For example, in low, stable pH conditions the coralline algae, *Lithothamnion glaciale*, increased its calcification rate relative to a control treatment but did not concurrently increase its rate of photosynthesis (Kamenos et al., 2013). Kamenos et al. (2013) suggest that the upregulation of calcification may limit photosynthetic efficiency. In the present study, the increase in G_{day} coincided with a decrease in net photosynthesis. Photosynthesizing calcifiers in the community may be partitioning their energetic resources more towards calcification and away from photosynthesis in order to maintain a positive calcification rate (Kamenos et al., 2013). (2) An alternative hypothesis is that the calcifiers may be adapted or acclimatized to high pCO_2 conditions (Johnson et al., 2014) and have not yet reached their threshold because the rubble was collected from a naturally high and variable pCO_2 environment (Guadayol et al., 2014).

We saw a decline in calcification and photosynthesis in the extreme pCO_2 × temperature condition. In prior studies, calcification has been shown to decline with climate stressors and the magnitude of decline differs across species (Kroeker et al., 2010; Pandolfi et al., 2011; Ries et al., 2009; Kroeker et al., 2013). The concurrent decline in photosynthesis and calcification (Figs. 3a and 4) suggests that non-photosynthesizing invertebrates in the community (such as bivalves) might be dominating the calcification signal in these conditions. This hypothesis would explain the pattern that we see in Fig. 4, where communities in the most extreme pCO_2 and temperature conditions are net respiring during the day while still maintaining a small, positive calcification rate.

G_{night} rates are more straightforward, decreasing linearly with pCO_2 and temperature (Figs. 3b and 4). Similarly, Andersson et al. (2009) saw an increase in dissolution under acidic conditions in a community of corals, sand, and CCA. Previous studies on

BGD
11, 12799–12831, 2014

individual bioeroder taxa have also found higher rates of bioerosion or dissolution in more acidic, higher temperature conditions (Wisshak et al., 2013; Fang et al., 2013; Reyes-Nivia et al., 2013; Tribollet et al., 2009; Wisshak et al., 2012). Studies, including the present one, that focused on community-level responses have consistently found that ocean acidification will increase dissolution rates on coral reefs (Andersson and Gledhill, 2013).

Dissolution was more strongly affected by Standardized Climate Change than calcification: this result is not surprising. Bioerosion, an important driver of dissolution, may be more sensitive to changes in ocean acidity than calcification, leading to net dissolution in high CO_2 waters. Many boring organisms excrete acidic compounds, which may be less metabolically costly in a low pH environmen. Erez et al. (2011) hypothesize that increased dissolution, rather than decreased calcification, maybe be the reason that net coral reef calcification is sensitive to ocean acidification. The results of this study support this hypothesis. Although G_{net} declines linearly with pCO_2-temperature, calcification (G_{day}) and dissolution (G_{night}) have distinct responses to Standardized Climate Change. Our results highlight the need to study the effects of climate stressors on both calcification and dissolution.

Author contribution. Conceived and designed the experiments: NJS MJD. Performed the experiments: NJS. Analyzed the data: NJS MJD. Wrote the paper: NJS MJD.

Acknowledgement. Thanks to I. Caldwell, R. Coleman, J. Faith, K. Hurley, J. Miyano, R. Maguire, D. Schar, J. Sziklay, and M. M. Walton for help in field collections and lab analyses and to R. Briggs from UH SOEST Lab for Analytical Chemistry. M. J. Atkinson, R. Gates, C. Jury, H. Putnam, and R. Toonen gave thoughtful advice throughout the project. Comments by F. Mackenzie improved this manuscript. This project was supported by a NOAA Nancy Foster Scholarship to N. J. S., a PADI Foundation Grant to N. J. S., and Hawaii SeaGrant 1847 to MJD. This is HIMB contribution #xxxx, Hawai'i SeaGrant contribution #xxx, and SOEST #xxxx.

BGD
11, 12799–12831, 2014

References

Andersson, A. J. and Gledhill, D.: Ocean acidification and coral reefs: effects on breakdown, dissolution, and net ecosystem calcification, Ann. Rev. Mar. Sci., 5, 321–348, 2013.

Andersson, A. J. and Mackenzie, F. T.: Revisiting four scientific debates in ocean acidification research, Biogeosciences, 9, 893–905, doi:10.5194/bg-9-893-2012, 2012.

Andersson, A. J., Kuffner, I. B., Mackenzie, F. T., Jokiel, P. L., Rodgers, K. S., and Tan, A.: Net Loss of $CaCO_3$ from a subtropical calcifying community due to seawater acidification: mesocosm-scale experimental evidence, Biogeosciences, 6, 1811–1823, doi:10.5194/bg-6-1811-2009, 2009.

Andersson, A. J., Mackenzie, F. T., and Gattuso, J.-P.: Effects of ocean acidification on benthic processes, organisms, and ecosystems, in: Ocean Acidification, edited by: Gattuso, J.-P. and Hansson, L., Oxford University Press, Oxford, 122–153, 2011.

Bopp, L., Resplandy, L., Orr, J. C., Doney, S. C., Dunne, J. P., Gehlen, M., Halloran, P., Heinze, C., Ilyina, T., Séférian, R., Tjiputra, J., and Vichi, M.: Multiple stressors of ocean ecosystems in the 21st century: projections with CMIP5 models, Biogeosciences, 10, 6225–6245, doi:10.5194/bg-10-6225-2013, 2013.

Caldeira, K. and Wickett, M. E.: Oceanography: anthropogenic carbon and ocean pH, Nature, 425, 365–365, 2003.

Comeau, S., Edmunds, P. J., Spindel, N. B., and Carpenter, R. C.: The responses of eight coral reef calcifiers to increasing partial pressure of CO_2 do not exhibit a tipping point, Limnol. Oceanogr, 58, 388–398, 2013.

Cubasch, U., Wuebbles, D., Chen, D., Facchini, M. C., Frame, D., Mahowald, N., and Winther, J.-G.: Climate Change 2013: The Physical Science Basis. Contribution of Working Group I to the Fifth Assessment Report of the Intergovernmental Panel on Climate Change Cambridge, UK and New York, NY, USA, 2013.

Diaz-Pulido, G., Anthony, K., Kline, D. I., Dove, S., and Hoegh-Guldberg, O.: Interactions between ocean acidification and warming on the mortality and dissolution of coralline alge, J. Phycol., 48, 32–39, 2012.

Dickson, A. G.: Standard potential of the reaction: AgCl (s)+ $12H_2$(g)= Ag (s)+ HCl (aq), and and the standard acidity constant of the ion HSO_4^- in synthetic sea water from 273.15 to 318.15 K, J. Chem. Thermodynam., 22, 113–127, 1990.

BGD
11, 12799–12831, 2014

Dickson, A. G. and Millero, F. J.: A comparison of the equilibrium constants for the dissociation of carbonic acid in seawater media, Deep-Sea Res. Pt.I, 34, 1733–1743, 1987.
Dickson, A. G., Sabine, C. L., and Christian, J. R.: Guide to best practices for ocean CO_2 measurements, PICES Special Publication 3, 191 pp., 2007.
Doney, S. C., Fabry, V. J., Feely, R. A., and Kleypas, J. A.: Ocean acidification: the other CO_2 problem, Ann. Rev. Mar. Sci., 1, 169–192, 2009.
Drupp, P. S., De Carlo, E. H., Mackenzie, F. T., Sabine, C. L., Feely, R. A., and Shamberger, K. E.: Comparison of CO_2 dynamics and air–sea gas exchange in differing tropical reef environments, Aquatic Geochem., 19, 371–397, 2013.
Erez, J., Reynaud, S., Silverman, J., Schneider, K., and Allemand, D.: Coral calcification under ocean acidification and global change, in: Coral Reefs: an Ecosystem in Transition, edited by: Dubinski, Z., and Stambler, N., Springer, 151–176, 2011.
Fabricius, K. E.: Effects of terrestrial runoff on the ecology of corals and coral reefs: review and synthesis, Mar. Pollut. Bull., 50, 125–146, 2005.
Fabricius, K., Langdon, C., Uthicke, S., Humphrey, C., Noonan, S., De'ath, G., Okazaki, R., Muehllehner, N., Glas, M., and Lough, J.: Losers and winners in coral reefs acclimatized to elevated carbon dioxide concentrations, Nature Climate Change, 1, 165–169, 2011.
Fair, R. C.: On the robust estimation of econometric models, Ann. Econ. Soc. Meas., 3, 117–128, 1974.
Fang, J. K. H., Mello-Athayde, M. A., Schönberg, C. H. L., Kline, D. I., Hoegh-Guldberg, O., and Dove, S.: Sponge biomass and bioerosion rates increase under ocean warming and acidification, Global Change Biol., 19, 3581–3591, 2013.
Fangue, N. A., O'Donnell, M. J., Sewell, M. A., Matson, P. G., MacPherson, A. C., and Hofmann, G. E.: A laboratory-based, experimental system for the study of ocean acidification effects on marine invertebrate larvae, Limnol. Oceanogr. Methods, 8, 441–452, 2010.
Feely, R. A., Sabine, C. L., Lee, K., Berelson, W., Kleypas, J., Fabry, V. J., and Millero, F. J.: Impact of anthropogenic CO_2 on the $CaCO_3$ system in the oceans, Science, 305, 362–366, 2004.
Findlay, H. S., Wood, H. L., Kendall, M. A., Spicer, J. I., Twitchett, R. J., and Widdicombe, S.: Comparing the impact of high CO_2 on calcium carbonate structures in different marine organisms, Mar. Biol. Res., 7, 565–575, 2011.

BGD
11, 12799–12831, 2014

Gattuso, J.-P., Frankignoulle, M., and Smith, S. V.: Measurement of community metabolism and significance in the coral reef CO_2 source-sink debate, Proc. Natl. Acad. Sci., 96, 13017–13022, 1999.
Guadayol, Ò., Silbiger, N. J., Donahue, M. J., and Thomas, F. I. M.: Patterns in temporal variability of temperature, oxygen and pH along an environmental gradient in a coral reef, PloS one, 9, e85213, doi:10.1371/journal.pone.0085213, 2014.
Hoegh-Guldberg, O. and Bruno, J. F.: The impact of climate change on the world's marine ecosystems, Science, 328, 1523–1528, 2010.
Hoegh-Guldberg, O., Mumby, P. J., Hooten, A. J., Steneck, R. S., Greenfield, P., Gomez, E., Harvell, C. D., Sale, P. F., Edwards, A. J., Caldeira, K., Knowlton, N., Eakin, C. M., Iglesias-Prieto, R., Muthiga, N., Bradbury, R. H., Dubi, A., and Hatziolos, M. E.: Coral reefs under rapid climate change and ocean acidification, Science, 318, 1737–1742, 2007.
Hurd, C. L., Cornwall, C. E., Currie, K., Hepburn, C. D., McGraw, C. M., Hunter, K. A., and Boyd, P. W.: Metabolically induced pH fluctuations by some coastal calcifiers exceed projected 22nd century ocean acidification: a mechanism for differential susceptibility?, Glob. Change Biol., 17, 3254–3262, 2011.
Johnson, M. D. and Carpenter, R. C.: Ocean acidification and warming decrease calcification in the crustose coralline alga *Hydrolithon onkodes* and increase susceptibility to grazing, J. Exp. Mar. Biol. Ecol., 434, 94–101, 2012.
Johnson, M. D., Moriarty, V. W., and Carpenter, R. C.: Acclimatization of the crustose coralline alga *Porolithon onkodes* to variable pCO_2, PLOS ONE, 9, e87678, doi:10.1371/journal.pone.0087678, 2014.
Jokiel, P. L., Rodgers, K. S., Kuffner, I. B., Andersson, A. J., Cox, E. F., and Mackenzie, F. T.: Ocean acidification and calcifying reef organisms: a mesocosm investigation, Coral Reefs, 27, 473–483, 2008.
Jury, C. P., Thomas, F. I. M., Atkinson, M. J., and Toonen, R. J.: Buffer capacity, ecosystem feedbacks, and seawater chemistry under global change, Water, 5, 1303–1325, 2013.
Kamenos, N. A., Burdett, H. L., Aloisio, E., Findlay, H. S., Martin, S., Longbone, C., Dunn, J., Widdicombe, S., and Calosi, P.: Coralline algal structure is more sensitive to rate, rather than the magnitude, of ocean acidification, Global Change Biology, 19, 3621–3628, 2013.
Kleypas, J. and Langdon, C.: Coral reefs and changing seawater chemistry, in: Coral Reefs and Climate Change: Science and Management, edited by: Phinney, J., Skirving, W., Kleypas, J., and Hoegh-Guldberg, O., American Geophysical Union, Washington D. C., 73–110, 2006.

BGD
11, 12799–12831, 2014

Kroeker, K. J., Kordas, R. L., Crim, R. N., and Singh, G. G.: Meta-analysis reveals negative yet variable effects of ocean acidification on marine organisms, Ecol. Lett., 13, 1419–1434, 2010.

Kroeker, K. J., Kordas, R. L., Crim, R., Hendriks, I. E., Ramajo, L., Singh, G. S., Duarte, C. M., and Gattuso, J. P.: Impacts of ocean acidification on marine organisms: quantifying sensitivities and interaction with warming, Glob. Change Biol., 19, 1884–1896, 2013.

Lowe, R. J., Falter, J. L., Monismith, S. G., and Atkinson, M. J.: A numerical study of circulation in a coastal reef-lagoon system, J. Geophys. Res.-Oceans, 114, C06022, doi:10.1029/2008JC005081, 2009a.

Lowe, R. J., Falter, J. L., Monismith, S. G., and Atkinson, M. J.: Wave-driven circulation of a coastal reef-lagoon system, J. Phys. Oceanogr., 39, 873–893, 2009b.

Martin, S., Cohu, S., Vignot, C., Zimmerman, G., and Gattuso, J. P.: One-year experiment on the physiological response of the Mediterranean crustose coralline alga, *Lithophyllum cabiochae*, to elevated pCO_2 and temperature, Ecol. Evol., 3, 676–693, 2013.

Mehrbach, C.: Measurement of the apparent dissociation constants of carbonic acid in seawater at atmospheric pressure, Limnol. Oceanogr., 18, 897–907, 1973.

Meinshausen, M., Smith, S. J., Calvin, K., Daniel, J. S., Kainuma, M. L. T., Lamarque, J. F., Matsumoto, K., Montzka, S. A., Raper, S. C. B., and Riahi, K.: The RCP greenhouse gas concentrations and their extensions from 1765 to 2300, Clim. Change, 109, 213–241, 2011.

Pandolfi, J. M., Connolly, S. R., Marshall, D. J., and Cohen, A. L.: Projecting coral reef futures under global warming and ocean acidification, Science, 333, 418–422, 2011.

Reyes-Nivia, C., Diaz-Pulido, G., Kline, D., Guldberg, O.-H., and Dove, S.: Ocean acidification and warming scenarios increase microbioerosion of coral skeletons, Glob. Change Biol., 19, 1919–1929, 2013.

Ries, J. B., Cohen, A. L., and McCorkle, D. C.: Marine calcifiers exhibit mixed responses to CO_2-induced ocean acidification, Geology, 37, 1131–1134, 2009.

Rodolfo-Metalpa, R., Houlbrèque, F., Tambutté, É., Boisson, F., Baggini, C., Patti, F. P., Jeffree, R., Fine, M., Foggo, A., and Gattuso, J. P.: Coral and mollusc resistance to ocean acidification adversely affected by warming, Nature Clim. Change, 1, 308–312, 2011.

Rogelj, J., Meinshausen, M., and Knutti, R.: Global warming under old and new scenarios using IPCC climate sensitivity range estimates, Nature Clim. Change, 2, 248–253, 2012.

Sanford, T., Frumhoff, P. C., Luers, A., and Gulledge, J.: The climate policy narrative for a dangerously warming world, Nature Clim. Change, 4, 164–166, 2014.

BGD
11, 12799–12831, 2014

Semesi, I. S., Kangwe, J., and Björk, M.: Alterations in seawater pH and CO_2 affect calcification and photosynthesis in the tropical coralline alga, *Hydrolithon sp.* (Rhodophyta), Estuarine, Coast. Shelf Sci., 84, 337–341, 2009.

Silbiger, N. J., Guadayol, Ò., Thomas, F. I. M., and Donahue M. J.: Reefs shift from net accretion to net erosion along a natural environmental gradient, Mar. Ecol. Progress Ser., in press, 2014.

Smith, S. V. and Key, G. S.: Carbon dioxide and metabolism in marine environments, Limnol. Oceanogr, 20, 493–495, 1975.

Smith, S. V., Kimmerer, W. J., Laws, E. A., Brock, R. E., and Walsh, T. W.: Kaneohe Bay sewage diversion experiment-perspectives on ecosystem responses to nutritional perturbation, Pacif. Sci., 35, 279–402, 1981.

Stimson, J. and Kinzie III, R. A.: The temporal pattern and rate of release of zooxanthellae from the reef coral *Pocillopora damicornis* (Linnaeus) under nitrogen-enrichment and control conditions, J. Exp. Mar. Biol. Ecol., 153, 63–74, 1991.

Tans, P. and Keeling, R.: NOAA/ESRL, available at: www.esrl.noaa.gov/gmd/ccgg/trends/, 2013.

Tribollet, A., and Payri, C.: Bioerosion of the coralline alga *Hydrolithon onkodes* by microborers in the coral reefs of Moorea, French Polynesia, Oceanol. Acta, 24, 329–342, 2001.

Tribollet, A., Atkinson, M. J., and Langdon, C.: Effects of elevated pCO_2 on epilithic and endolithic metabolism of reef carbonates, Glob. Change Biol., 12, 2200–2208, 2006.

Tribollet, A., Godinot, C., Atkinson, M., and Langdon, C.: Effects of elevated pCO_2 on dissolution of coral carbonates by microbial euendoliths, Global Biogeochem. Cy., 23, GB3008, 2009.

Uppström, L. R.: The boron/chlorinity ratio of deep-sea water from the Pacific Ocean, Deep Sea Research and Oceanographic Abstracts, 1974, 161–162.

Van Heuven, S., Pierrot, D., Lewis, E., and Wallace, D. W. R.: MATLAB Program developed for CO_2 system calculations, Rep. ORNL/CDIAC-105b, 2009.

Van Vuuren, D. P., Meinshausen, M., Plattner, G. K., Joos, F., Strassmann, K. M., Smith, S. J., Wigley, T. M. L., Raper, S. C. B., Riahi, K., and De La Chesnaye, F.: Temperature increase of 21st century mitigation scenarios, Proc. Natl. Acad. Sci., 105, 15258–15262, 2008.

Van Vuuren, D. P., Edmonds, J., Kainuma, M., Riahi, K., Thomson, A., Hibbard, K., Hurtt, G. C., Kram, T., Krey, V., and Lamarque, J.-F.: The representative concentration pathways: an overview, Clim. Change, 109, 5–31, 2011.

BGD
11, 12799–12831, 2014

White, J.: Distribution, recruitment and development of the borer community in dead coral on shallow Hawaiian reefs, Ph. D., Zoology, University of Hawaii at Manoa, Honolulu, 1980.
Wisshak, M., Schönberg, C. H. L., Form, A., and Freiwald, A.: Ocean acidification accelerates reef bioerosion, Plos One, 7, e45124–e45124, 2012.
Wisshak, M., Schönberg, C. H. L., Form, A., and Freiwald, A.: Effects of ocean acidification and global warming on reef bioerosion – lessons from a clionaid sponge, Aq. Biol., 19, 111–127, 2013.
Yates, K. K. and Halley, R. B.: CO_3^{2-} concentration and pCO_2 thresholds for calcification and dissolution on the Molokai reef flat, Hawaii, Biogeosciences, 3, 357–369, doi:10.5194/bg-3-357-2006, 2006.

BGD
11, 12799–12831, 2014

Table 1. Means and standard errors of all measured parameters by rack. pCO_2, HCO_3^-, CO_3^{2-}, DIC, and Ω_{arag} were all calculated from the measured TA and pH samples using CO2SYS. Data are all from the imposed treatment conditions with no rubble inside the aquaria.

Rack	Pre-industrial	Present Day	2050 prediction	2100 prediction
Temp (°C)	23.8 ± 0.07	24.8 ± 0.08	26.2 ± 0.06	27.2 ± 0.08
Salinity (psu)	35.65 ± 0.01	35.71 ± 0.02	35.62 ± 0.02	35.71 ± 0.02
Total Alkalinity (μmol kg^{-1})	2137 ± 1.7	2138 ± 2.3	2139 ± 2.0	2142 ± 1.9
pH_t	8.02 ± 0.02	7.87 ± 0.01	7.74 ± 0.02	7.67 ± 0.02
pCO_2 (μatm)	409 ± 20.0	614 ± 15.6	868 ± 33.0	1047 ± 38.7
HCO_3^- (μmol kg^{-1})	1692 ± 16.9	1815 ± 7.3	1894 ± 7.8	1939 ± 6.6
CO_3^{2-} (μmol kg^{-1})	194.20 ± 6.7	147.08 ± 2.8	113.98 ± 3.8	99.24 ± 3.3
DIC (μmol kg^{-1})	1898 ± 10.9	1980 ± 5.1	2032 ± 5.0	2067 ± 4.5
Ω_{arag}	3.06 ± 0.1	2.32 ± 0.04	1.80 ± 0.06	1.57 ± 0.05
NO_2^- (μmol L^{-1})	0.082 ± 0.0028	0.078 ± 0.0045	0.074 ± 0.0047	0.070 ± 0.0051
PO_4^{3-} (μmol L^{-1})	0.017 ± 0.014	0.0097 ± 0.0081	0.033 ± 0.016	0.018 ± 0.0061
$Si(OH)_4$ (μmol L^{-1})	3.60 ± 0.58	3.64 ± 0.61	3.88 ± 0.49	3.78 ± 0.52
NH_4^+ (μmol L^{-1})	0.45 ± 0.30	0.19 ± 0.067	0.23 ± 0.15	0.34 ± 0.14
NO_3^- (μmol L^{-1})	2.13 ± 0.20	2.25 ± 0.21	2.55 ± 0.10	2.48 ± 0.11

BGD
11, 12799–12831, 2014

Table 2. Regression results for the treatment experiments: G_{day}, G_{night}, and G_{net} versus Standardized Climate Change (Fig. 3).

	SS	d*f*	F	*p*	R^2
G_{day}					
Standardized Climate Change	5.82	1	1.97	0.17	
(Standardized Climate Change)^2	18.67	1	6.33	**0.02**	
Error	61.86	21	2.95		0.29
G_{night}					
Standardized Climate Change	73.60	1	50.09	< **0.0001**	
Error	32.32	22			0.70
G_{net}					
Standardized Climate Change	89.79	1	20.25	< **0.001**	
Error	97.57	22	0.002		0.48

BGD
11, 12799–12831, 2014

Table A1. Analysis of treatment experiment using an ANOVA design (Appendix Fig. A4).

	SS	df	MS	F	*p*
G_{day}					
Groups	28.83	3	9.81	3.65	**0.030**
Error	52.61	20	2.63		
Total	81.45	23			
G_{night}					
Groups	60.39	3	20.13	8.84	< **0.0001**
Error	45.53	20	2.28		
Total	105.92	23			
G_{net}					
Groups	104.31	3	34.77	8.37	< **0.0001**
Error	83.05	20	4.15		
Total	197.36	23			

BGD
11, 12799–12831, 2014

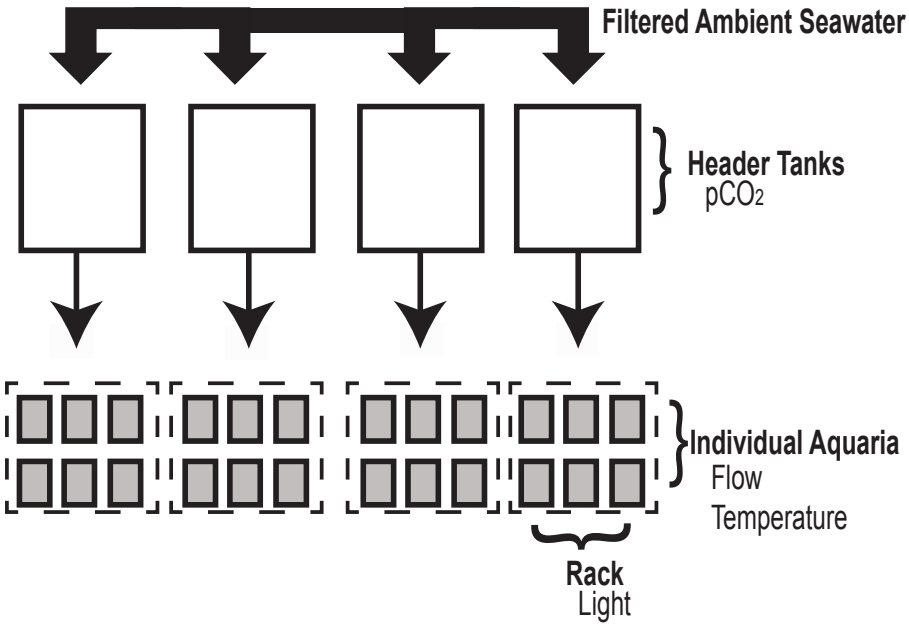

Figure 1. A schematic of the mesocosm system at the Hawai'i Institute of Marine Biology. Ambient seawater is pumped into the system from a nearby fringing reef in Kāne'ohe Bay. The seawater is filtered with a sand trap filter, passed through a water chiller and then fed into one of four header tanks. pCO_2 is manipulated in each header tank by bubbling a mixture of CO_2-free air and pure CO_2 to the desired concentration. The water from one header tank flows into 6 aquaria (a rack). Light is controlled by rack with metal-halide lights. There are two metal-halide lights per rack with each light oscillating over a set of three aquaria. Flow and temperature are controlled in each individual aquarium with flow valves and aquarium heaters, respectively.

BGD
11, 12799–12831, 2014

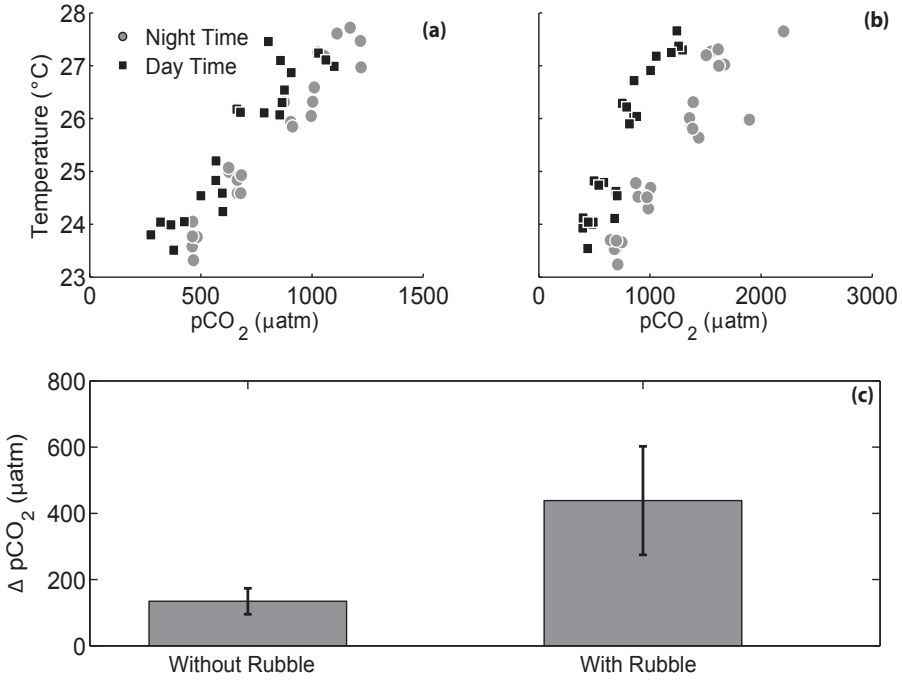

Figure 2. pCO_2 and temperature in each aquarium **(a)** without any rubble present and **(b)** with rubble present. Daily variability in pCO_2 was higher when rubble was present due to feedbacks from the rubble community. (Note the different x axis scales in panels **a** and **b**). Panel **(c)** shows the mean difference between day and night pCO_2 with and without rubble present (error bars are standard error) ($t_{23} = -7.23$, $p < 0.0001$).

BGD
11, 12799–12831, 2014

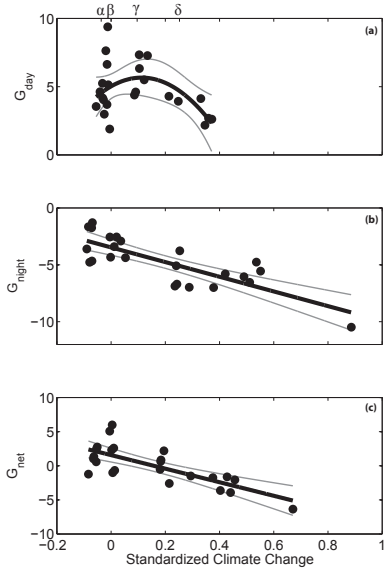

Figure 3. Net ecosystem calcification: **(a)** G_{day}, **(b)** G_{night}, and **(c)** G_{net} versus Standardized Climate Change. Each point represents net ecosystem calcification calculated from an individual aquarium. Standardized Climate Change was centered around background seawater conditions such that a value of 0 indicated that there was no change in pCO_2 or temperature. Positive values indicate an elevated pCO_2 and temperature condition relative to background and negative values represent lower pCO_2 and temperature conditions. G_{day} had a non-linear relationship with Standardized Climate Change ($y = -1.6 \times 10^{-8}x^2 + 1.4 \times 10^{-4}x + 5.5$), while G_{night} ($y = -1.3 \times 10^{-4}x - 3.4$) and G_{net} ($y = -1.7 \times 10^{-4}x + 1.4$) each had a negative linear relationship with Standardized Climate Change (Table 2). Black lines are best fit lines for each model with 95 % confidence intervals in gray. Greek letters on the top panel represent the imposed conditions for pre-industrial (α), present day (β), 2050 (γ), and 2100 (δ).

BGD
11, 12799–12831, 2014

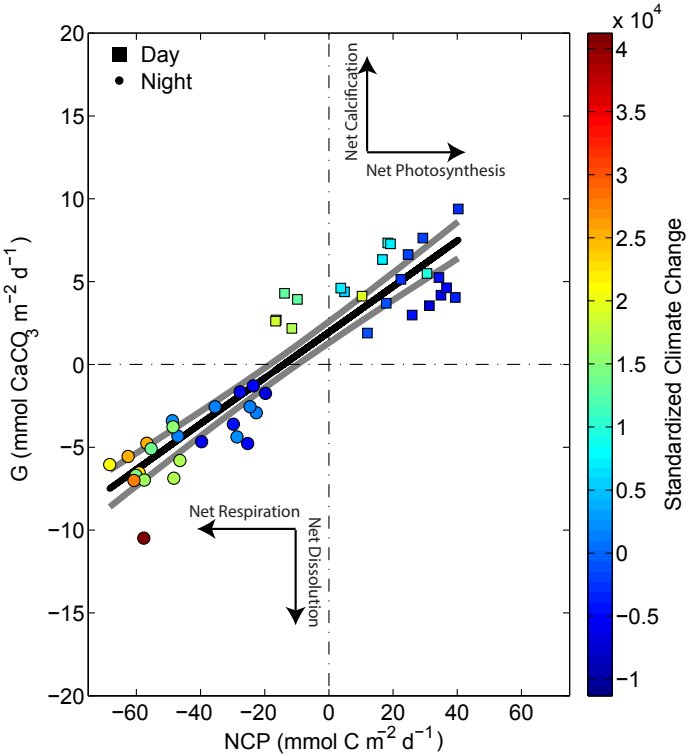

Figure 4. Calculated *G* and NCP rates for all treatment aquaria. The color represents Standardized Climate Change. Squares are data collected during the light conditions and circles represent data collected during dark conditions. All negative numbers are either net dissolution or net respiration while positive numbers are net calcification or net photosynthesis. There is a strong positive relationship between *G* and NCP ($y = 0.14x + 1.9$, $p < 0.0001$, $R^2 = 0.85$). Black and gray lines represent the best-fit line and 95 % confidence intervals, respectively. Supplement Fig. A3 is a similar plot with specific aquaria labeled.

BGD
11, 12799–12831, 2014

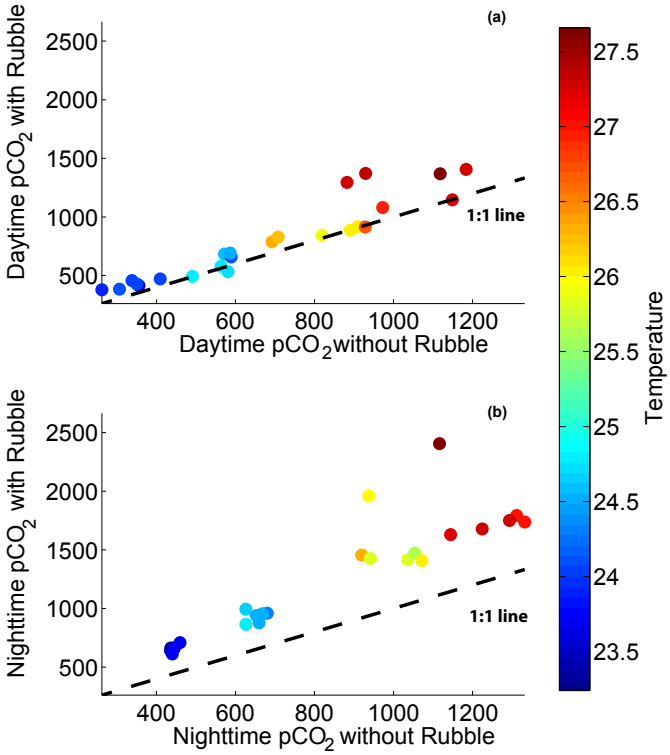

Figure A1. Feedbacks in seawater chemistry caused by the presence of rubble during the day and night. *x* axis is pCO_2 in seawater without any rubble and *y* axis is pCO_2 in seawater with rubble present. Color represents temperature. The top panel is data collected during the day and the bottom panel is data collected at night. The black line is a 1 : 1 line. The pCO_2 conditions drift farther away from the manipulated conditions during the night.

BGD
11, 12799–12831, 2014

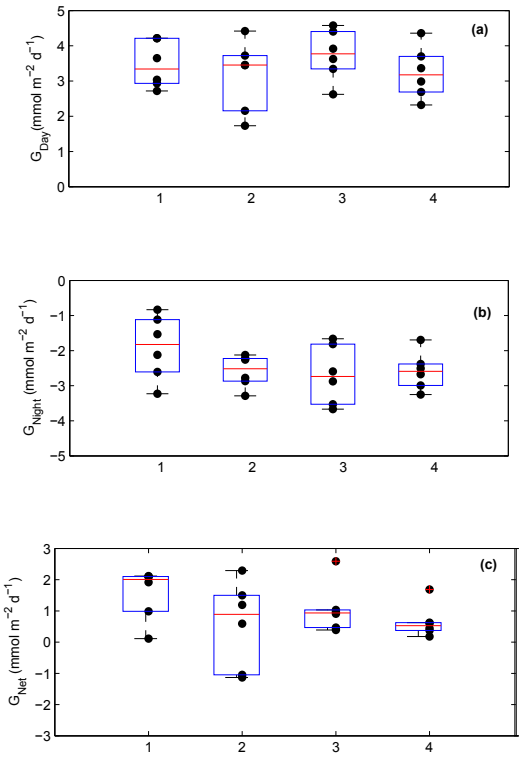

Figure A2. Boxplots for **(a)** G_{day}, **(b)** G_{night}, and **(c)** G_{net} for the control experiment, separated by rack. We used an ANOVA to test for differences across racks and found no significant difference in G_{day} ($F_{3,23}$ = 0.68, p = 0.58), G_{night} ($F_{3,23}$ = 1.52, p = 0.24), or G_{net} ($F_{3,23}$ = 1.38, p = 0.28).

BGD
11, 12799–12831, 2014

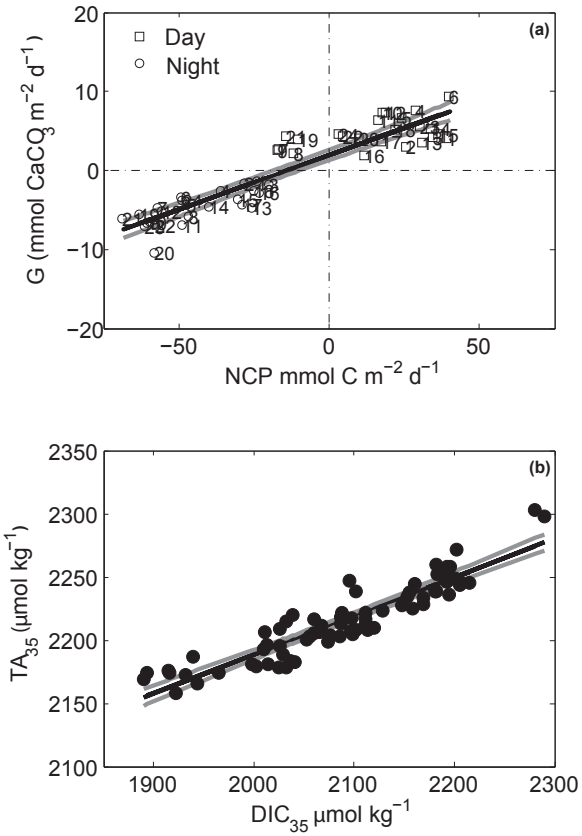

Figure A3. Panel **(a)** is G versus NCP rates numbered by tank. Data and best fit line are the same as Fig. 4. Panel **(b)** is salinity normalized TA on the y axis and salinity normalized DIC on the x axis in µmol kg^{-1}. There is a strong positive relationship between TA and DIC ($y = 0.31x + 0.0016$, $p < 0.0001$, $R^2 = 0.85$).

BGD
11, 12799–12831, 2014

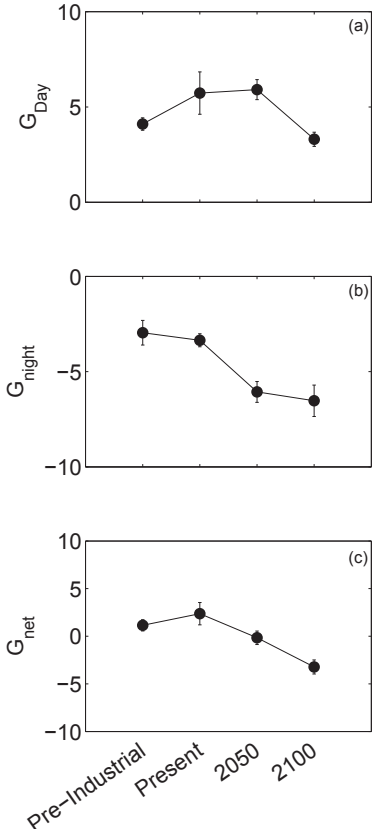

Figure A4. Means and standard error bars for **(a)** G_{day}, **(b)** G_{night}, and **(c)** G_{net} in mmol m^{-2} d^{-1}. x axis represents climate scenario treatments. There were significant differences across treatments for G_{day} ($p = 0.03$), G_{night} ($p < 0.0001$), and G_{net} ($p < 0.0001$) (Table A1).

BGD
11, 12799–12831, 2014